

RM-synthesis of the Perseus cluster

M.A. Brentjens^{1,2,*} and A.G. de Bruyn^{2,1}

¹ Kapteyn Astronomical Institute, University of Groningen, P.O. Box 800, 9700 AV Groningen, the Netherlands

² ASTRON, P.O. Box 2, 7990 AA Dwingeloo, the Netherlands

Received 2006 Mar 15, accepted 2006 Mar 21

Published online 2006 May 11

Key words galaxies: clusters: general – galaxies: active – polarization – magnetic fields – techniques: image processing – radio continuum: general

We present low frequency radio polarimetric observations of the Perseus cluster. The data were taken with the Westerbork Synthesis Radio Telescope (WSRT) between 315–360 MHz. We have discovered faint, extended, highly polarized emission that we associate with the Perseus cluster (de Bruyn & Brentjens 2005). We propose that at least one of these structures is associated with large-scale structure formation gas inflow from the Perseus-Pisces supercluster. The extragalactic emission is seen through a polarized Galactic synchrotron foreground screen. The discovery was made possible by a novel rotation measure analysis technique, called Faraday Rotation Measure Synthesis, or RM-synthesis for short (Brentjens & de Bruyn 2005).

© 2006 WILEY-VCH Verlag GmbH & Co. KGaA, Weinheim

1 Introduction

Clusters of galaxies are found at the intersections of long, relatively high density supercluster filaments, along which smaller clusters and galaxy groups flow towards the clusters. The clusters and the filaments connecting them form the so-called cosmic web (Bond et al. 1996).

The central regions of clusters contain extremely hot gas that is easily observed in X-rays. However, the gas density and temperature decrease with increasing distance from the cluster centre, rendering the gas almost invisible at large distances in even the most sensitive X-ray observations (Kaastra et al. 2003). Supercluster filaments show up as strings of galaxies in large galaxy-redshift surveys like the Sloan Digital Sky Survey (SDSS) and the 2dF redshift survey. All cosmological simulations show that there must be a significant amount of gas in these filaments. There should be large Mpc-scale shock fronts where the gas flow from the supercluster impacts on the cluster intergalactic medium (IGM) (e.g. Burns 1998).

We present observations of the Perseus cluster that reveal large, diffuse, highly polarized structures at the interface with the Perseus-Pisces supercluster. In Sec. 2 we briefly discuss the technique of Faraday Rotation Measure Synthesis. The observations are described in Sec. 3. The nature of the observed features is discussed in Sec. 4. In Sec. 5 we estimate a lower limit to the magnetic field strength at a distance of 1 to 2 Mpc from the cluster centre. Section 6 concludes.

Assuming $H_0 = 72 \pm 2 \text{ km s}^{-1} \text{ Mpc}^{-1}$ (Spergel et al. 2003), 1° on the sky corresponds to 1.5 Mpc at the Perseus cluster.

* Corresponding author: m.a.brentjens@astro.rug.nl

2 RM-synthesis

Before proceeding to the observations, we briefly discuss the data analysis technique we used, called RM-synthesis. For details we refer to Brentjens & de Bruyn (2005). First we introduce some terminology. Following Burn (1966), we make a clear distinction between rotation measure (RM) and Faraday depth (ϕ). The Faraday depth of a source is given by

$$\phi(\mathbf{r}) = 0.81 \int_{\mathbf{r}}^{\text{here}} n_e \mathbf{B} \, dl \quad \text{rad m}^{-2}, \quad (1)$$

where n_e is the electron density in cm^{-3} , \mathbf{B} is the magnetic induction in μG , and dl is an infinitesimal path length in parsecs. We define the RM as

$$\text{RM}(\lambda^2) = \frac{d\chi(\lambda^2)}{d\lambda^2}, \quad (2)$$

where χ is the polarization position angle:

$$\chi = \frac{1}{2} \tan^{-1} \frac{U}{Q}. \quad (3)$$

In general, the RM of a source is *not* equal to its ϕ . They are only equal in special cases, such as sources that have negligible internal Faraday rotation, and sources without beam depolarization. In most other cases, the RM is not equal to ϕ . For a detailed discussion, see Brentjens & de Bruyn (2005).

It is useful to introduce the complex linearly polarized flux P , which can be written as

$$P = pI = Q + iU = \|p\| I e^{2i\chi}. \quad (4)$$

In Eq. (4), I , Q , and U are Stokes parameters, and p is the complex linear polarization fraction.

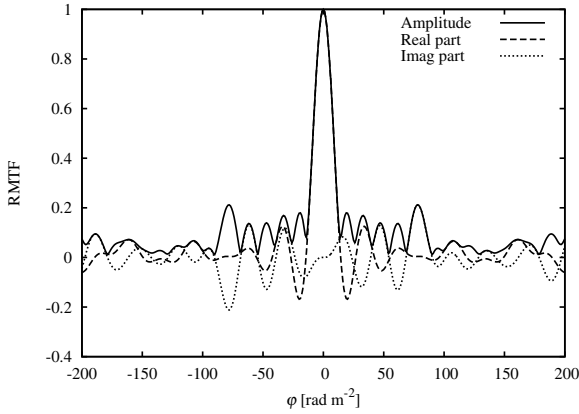


Fig. 1 The RMTF of the observations. The real part is the response parallel to the polarization vector at λ_0^2 and the imaginary part is the orthogonal response.

Burn (1966) also introduces the complex Faraday dispersion function $F(\phi)$, which is the complex linearly polarized surface brightness per unit Faraday depth, for example per (rad m^{-2}) or per rmtf^1 (the rotation measure transfer function, see next paragraph). It is defined through

$$P(\lambda^2) = \int_{-\infty}^{+\infty} F(\phi) e^{2i\phi\lambda^2} d\phi. \quad (5)$$

Equation (5) is invertible if one multiplies the righthand side by a weight function $W(\lambda^2)$ that is zero at $\lambda^2 < 0$ and at all other λ^2 at which data are missing. The inverse is

$$\tilde{F}(\phi) = F(\phi) * R(\phi) = K \int_{-\infty}^{+\infty} \tilde{P}(\lambda^2) e^{-2i\phi\lambda^2} d\lambda^2, \quad (6)$$

$$R(\phi) = K \int_{-\infty}^{+\infty} W(\lambda^2) e^{-2i\phi\lambda^2} d\lambda^2, \quad (7)$$

$$K = \left(\int_{-\infty}^{+\infty} W(\lambda^2) d\lambda^2 \right)^{-1}. \quad (8)$$

A tilde denotes either observed or reconstructed quantities. $\tilde{F}(\phi)$ is an approximate reconstruction of $F(\phi)$. More precisely, it is given by $F(\phi)$ convolved with $R(\phi)$ after Fourier filtering by $W(\lambda^2)$. The quality of the reconstruction depends mainly on $W(\lambda^2)$. Holes in the λ^2 sampling increase the side lobes of $R(\phi)$. Covering a larger range of λ^2 increases the resolution in ϕ space. The function $R(\phi)$ is called the rotation measure transfer function (RMTF). The RMTF of our observations is shown in Fig. 1.

Applying Eq. (6) with a given $\phi = \phi_k$ to all pixels in a map, using as many channel maps as possible for input, gives a map of the sky that is optimized for the detection of emission with $\phi = \phi_k$. One may repeat this exercise for a sequence of plausible ϕ_k to generate a RM-cube. That is, a data cube with axes α , δ , and ϕ , and value $\tilde{F}(\phi_k)$.

¹ When set in lower case, rmtf is used as a unit of Faraday depth, as in “1 Jy beam⁻¹ rmtf^{-1} ”. If RMTF is written in upper case, it refers to the function $R(\phi)$.

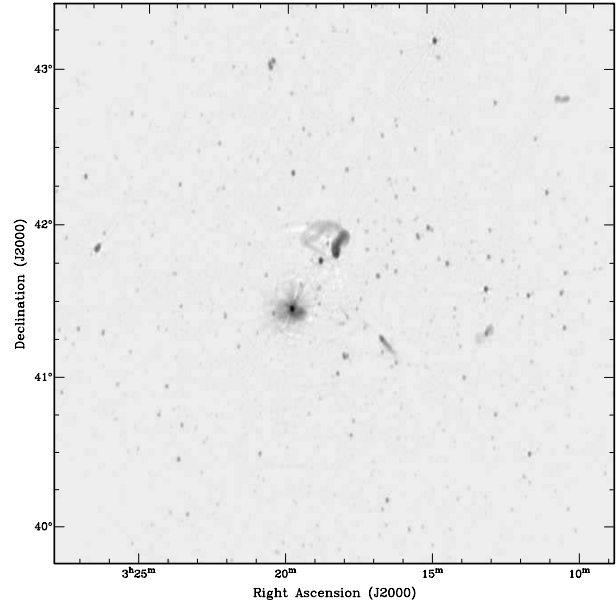


Fig. 2 Total intensity image of the Perseus cluster, observed with the WSRT in 2002, using data from band 3. The total bandwidth in the image is 8 MHz. The total integration time is 6×12 hours.

In short, RM-synthesis is an unbiased, unambiguous method to determine spatially varying RMs in cases of multiple rotations within the full recording bandwidth. In particular it can separate diffuse foreground emission from diffuse background emission through their difference in ϕ . RM-synthesis is currently the only method that can deliver a reliable RM if a detection of polarized signal per channel is not possible.

3 Observations

The observations were done with the Westerbork Synthesis Radio Telescope (WSRT). The telescope is an East-West array of fourteen 25 m parabolic dishes. The maximum baseline is 3 km, yielding a resolution of $\approx 1' \times 1.5'$ (RA \times DEC) at 90 cm wavelength. The resolution in Figs. 2 and 3 is $2' \times 3'$ (RA \times DEC).

We observed for 6×12 hours. There were 126 usable frequency channels between 315 and 360 MHz. The theoretical noise limit, taking into account the data that we had to discard due to man made interference and malfunctioning hardware is about $50 \mu\text{Jy beam}^{-1}$. The noise level that we achieved in the RM-cube (Fig. 3) is about $70 \mu\text{Jy beam}^{-1} \text{rmtf}^{-1}$. This is much better than the classical confusion noise of about $1.5 \text{ mJy beam}^{-1}$ in Stokes I for this frequency and resolution. The images in Fig. 3 are the deepest low frequency polarization radio maps ever constructed.

Figure 3 shows four frames from the RM-cube of the Perseus cluster. The grey scale is $\|F(\phi)\|$, which can be regarded as the total linearly polarized flux per unit ϕ , in this case: per rmtf . For orientation, Fig. 2 shows a total intensity image of the same area at the same scale as Fig. 3.

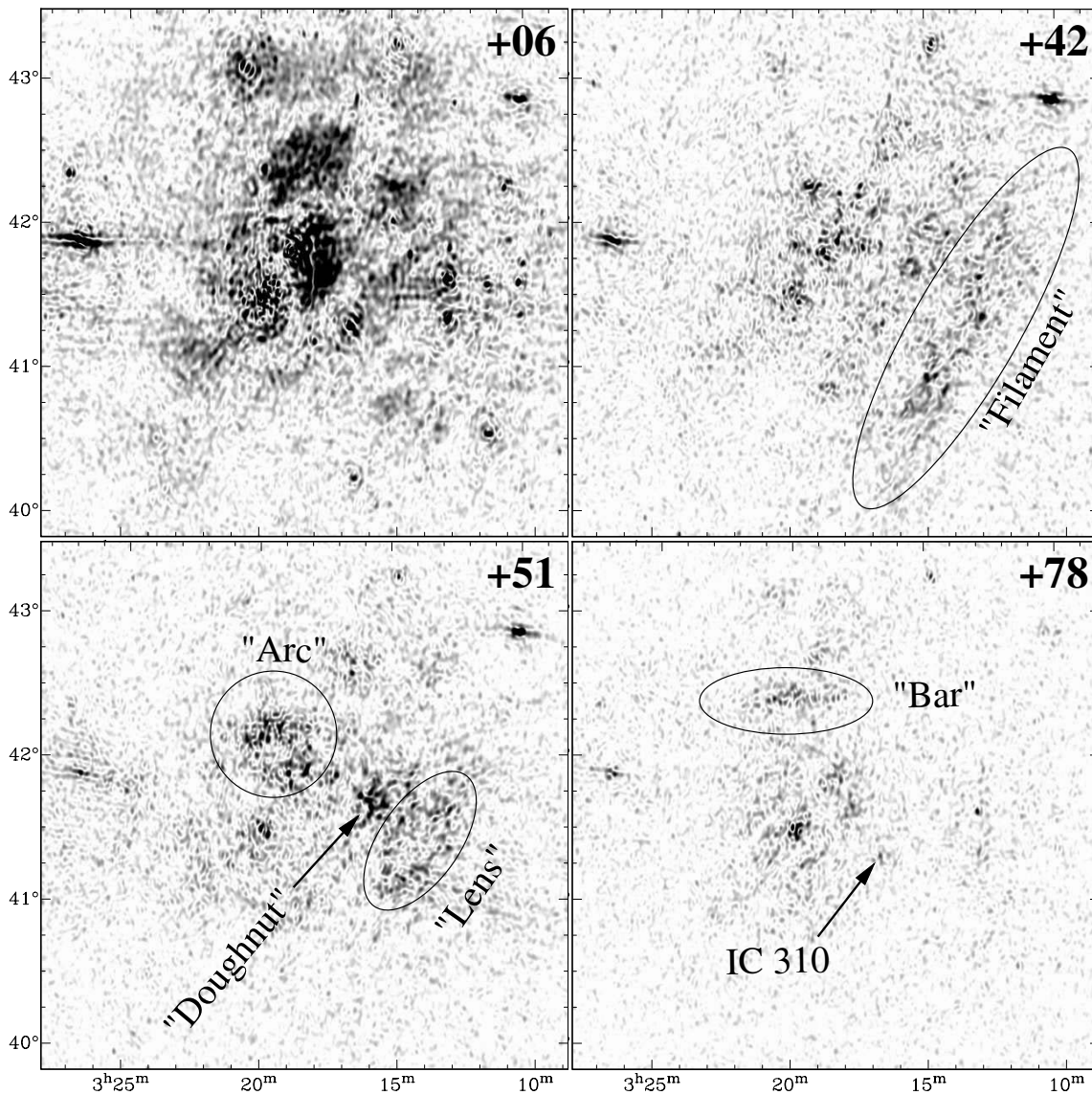


Fig. 3 Four characteristic frames from the RM-cube. The grey scale is $\|\tilde{F}(\phi)\|$. The Faraday depth of each frame is specified in the top right corner in rad m^{-2} .

The brightness of Fig. 2 is logarithmically scaled in order to compress the dynamic range. A triangle of bright, extended sources dominates the field centre: NGC 1275 at the lower left, NGC 1265 at the top, and IC 310 at the lower right. Due to residual calibration errors, NGC 1275 is visible in all frames of the RM-cube. IC 310 shows up in the bottom right panel of Fig. 3 at $\phi \approx +80 \text{ rad m}^{-2}$.

The top left frame of Fig. 3 shows patches of Galactic synchrotron foreground emission. In the full RM-cube it is most prominent between $+6$ and $+12 \text{ rad m}^{-2}$, which is a fairly typical Faraday depth for Galactic synchrotron at these Galactic latitudes (Haverkorn et al. 2003). There is little emission between $\phi = +15$ and $+30 \text{ rad m}^{-2}$.

The features at $\phi > 30 \text{ rad m}^{-2}$ are much more motled than the Galactic foreground. The frame at $\phi = +42 \text{ rad m}^{-2}$ shows a large, straight feature, labelled ‘‘Fila-

ment’’. It is located at the western side of the Perseus cluster. It is approximately $2^\circ 40'$ long, which corresponds to about 3.5 Mpc at the distance of the cluster. It is of the order of 200 kpc wide. The ‘‘Filament’’ aligns almost perfectly with the major axis of the feature called ‘‘Lens’’ in the next frame. The ‘‘Lens’’ measures $1 \times 0.5 \text{ Mpc}$. North-East of the ‘‘Lens’’ is a bright ($2 \text{ mJy beam}^{-1} \text{ rmtf}^{-1}$) knot named ‘‘Doughnut’’. Its diameter is of the order of 200 to 300 kpc. Directly North of the steep spectrum tail of NGC 1265 (Sjobering & de Bruyn 1998) floats a large, curved structure called ‘‘Arc’’. The ‘‘Bar’’ in the last frame looks like the ‘‘Filament’’ of the second frame, except that it is a bit smaller (roughly $900 \times 100 \text{ kpc}$). We have seen no significant emission at $\phi > 85 \text{ rad m}^{-2}$.

None of the structures is visible in Stokes I . The brightest structure is the ‘‘Doughnut’’ with $\|\tilde{F}(\phi)\| \approx$

2 mJy beam⁻¹ rmtf⁻¹. Given a Stokes I noise level of 1.5 mJy beam⁻¹, that would imply a polarization percentage of over 100%. We have indications that the Stokes I emission of the cluster is rather smooth, rendering it invisible at all but the shortest spacings. On the other hand, the polarized emission is highly structured. Considering that the shortest spacing was unavailable in several frequency bands, it is likely that the actual polarization percentage is a factor of 2–3 lower, making it high (> 20–40%), but plausible.

4 What are these structures?

We believe that the structures at $\phi > 30 \text{ rad m}^{-2}$ are associated with the Perseus cluster for two reasons. The first is that they have a fairly constant ϕ excess of about 40–50 rad m⁻² with respect to the Galactic Faraday rotation determined from a mini RM-survey of extragalactic sources around the Perseus cluster (de Bruyn & Brentjens 2005). If a Galactic plasma cloud above the Perseus arm would cause the excess, it should have an electron density of the order of 0.8 cm⁻³, assuming a diameter of 60 pc and a magnetic field strength of 1 μG . Such a cloud should have an H α brightness of about 13 Rayleigh. The total H α surface brightness in WHAM (Haffner et al. 2003) is only 3–5 Rayleigh over an area of 3° × 3° centred on the Perseus cluster. The Perseus arm model for the origin of the excess Faraday rotation therefore appears to be untenable. The second reason is that the “Filament” and the “Bar” are very similar to the huge, highly polarized filaments found by Govoni et al. (2005) in Abell 2255.

The “Filament”, the “Bar”, and the filaments in Abell 2255 could be related to large-scale structure (LSS) formation infall onto the clusters. The “Filament” is located at the interface with the Perseus-Pisces supercluster. The fact that the “Lens” appears compressed and lines up almost perfectly with the “Filament”, suggests that the “Filament” is related to a giant shock wave. The “Lens” would then be a gigantic bubble in the IGM, possibly injected by ancient AGN activity (Enßlin et al. 1998; Enßlin & Brüggen 2002; Enßlin & Gopal-Krishna 2001). The “Doughnut” may be injected more recently. The “Arc” is tantalizingly similar in curvature to the steep spectrum tail of NGC 1265. Furthermore, it is situated directly “above” this tail. Could this be a previous, detached tail of NGC 1265?

5 A magnetic field estimate

One can estimate a lower limit to the magnetic field in the cloud that performs the Faraday rotation. This cloud must be *in front* of the polarized structures described in Sect. 3. We already established that the cloud cannot be part of the Galaxy. We assume that $\|\Delta\mathbf{l}\| \approx 2 \text{ Mpc}$ and $n_e \approx 10^{-4} \text{ cm}^{-3}$. We also assume a constant, homogeneous magnetic field along the line of sight. Given an excess of order +40 rad m⁻², we can estimate

$$\|\mathbf{B}\| \geq \phi / (0.8 n_e \|\Delta\mathbf{l}\|) = 0.3 \mu\text{G}. \quad (9)$$

This is a lower limit. In reality, the magnetic field is probably somewhat tangled, so it may not point directly towards us. Furthermore, the line of sight may be considerably shorter than 2 Mpc.

6 Conclusions

RM-synthesis enables the detection of weak, polarized emission by eliminating bandwidth depolarization. Furthermore, one can separate polarized foreground structures from background structures through the difference in ϕ . We believe that RM-synthesis is vital for the success of the SKA “Magnetic Universe” science case. It is an excellent tool to study magnetic properties of the IGM in the outskirts of galaxy clusters and beyond. Magnetic structure formation codes have never before been tested in this regime.

We have discovered weak, highly polarized, diffuse emission that is associated with the Perseus cluster. We tentatively conclude that the large, straight features are related to LSS shocks at the interface between the Perseus cluster and the Perseus-Pisces supercluster (“Filament”) and possibly to infall from the North (“Bar”). The straight features are similar in size and morphology to the filaments found near Abell 2255 by Govoni et al. (2005). The next step would be to trace these shocks well into the supercluster filaments. This may already be possible with current telescopes, however, LOFAR and the SKA will undoubtedly reveal many LSS shocks throughout the cosmic web.

Acknowledgements. The Westerbork Synthesis Radio Telescope is operated by ASTRON (Netherlands Foundation for Research in Astronomy) with support from the Netherlands Foundation for Scientific Research (NWO). The Wisconsin H-Alpha Mapper is funded by the National Science Foundation.

References

- Bond, J.R., Kofman, L., Pogosyan, D.: 1996, *Nature* 380, 603
- Brentjens, M.A., de Bruyn, A.G.: 2005, *A&A* 441, 1217
- Burn, B.J.: 1966, *MNRAS* 133, 67
- Burns, J.O.: 1998, *Science* 280, 400
- de Bruyn, A.G., Brentjens, M.A.: 2005, *A&A* 441, 931
- Enßlin, T.A., Biermann, P.L., Klein, U., Kohle, S.: 1998, *A&A* 332, 395
- Enßlin, T.A., Brüggen, M.: 2002, *MNRAS* 331, 1011
- Enßlin, T.A., Gopal-Krishna.: 2001, *A&A* 366, 26
- Govoni, F., Murgia, M., Feretti, L., et al.: 2005, *A&A* 430, L5
- Haffner, L.M., Reynolds, R.J., Tufte, S.L., et al.: 2003, *ApJS* 149, 405
- Haverkorn, M., Katgert, P., de Bruyn, A.G.: 2003, *A&A* 403, 1045
- Kaastra, J.S., Lieu, R., Tamura, T., Paerels, F.B.S., den Herder, J.W.: 2003, *A&A* 397, 445
- Sijbring, D., de Bruyn, A.G.: 1998, *A&A* 331, 901
- Spergel, D.N., Verde, L., Peiris, H.V., et al.: 2003, *ApJS* 148, 175